University of Colorado Boulder

Lunar Surface Assessment Tool (LSAT): A Simulation of Lunar Dust Dynamics for Risk Analysis

Amrita Singh (Graduate Student, Aerospace Engineering)
Gabriella Schauss (Graduate Student, Aerospace Engineering)
Faculty Advisors: Dr. James Nabity (primary), Dr. Allison Hayman

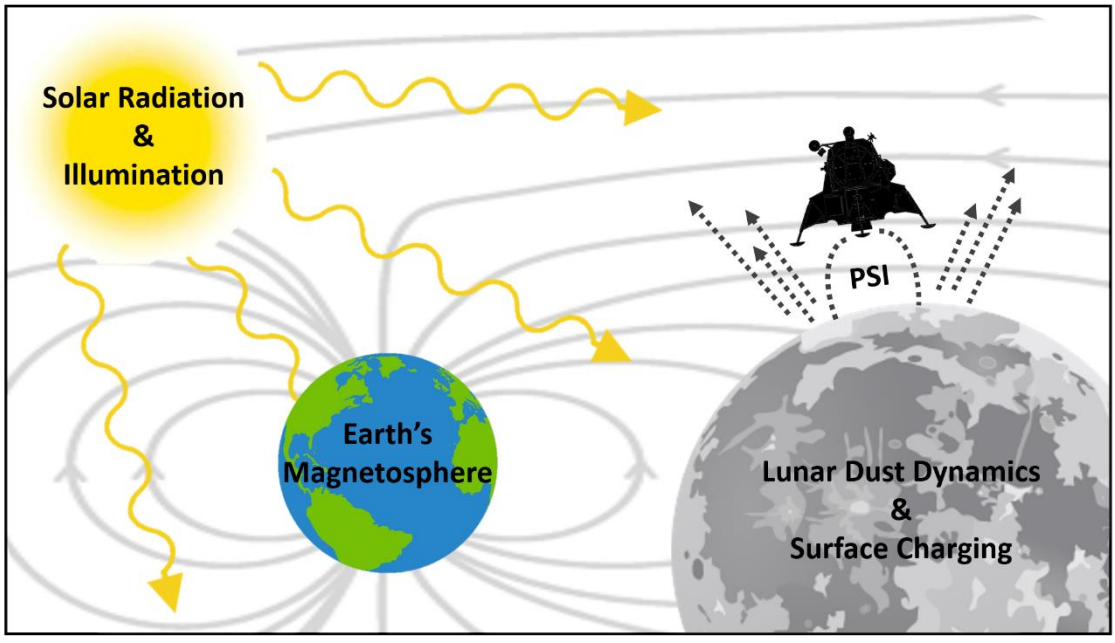

University of Colorado Boulder, Lunar Surface Assessment Tool (LSAT)

Major Objectives & Technical Approach

- Develop a holistic lunar dust dynamics simulation that considers the lunar surface electric potential as it varies due to topography, illumination condition, mission timing, and the presence of the Human Landing System (HLS).
- Integrate several first-principles models for charging in the plasma environment, solar illumination angle, and Plume-Surface Interactions (PSI).

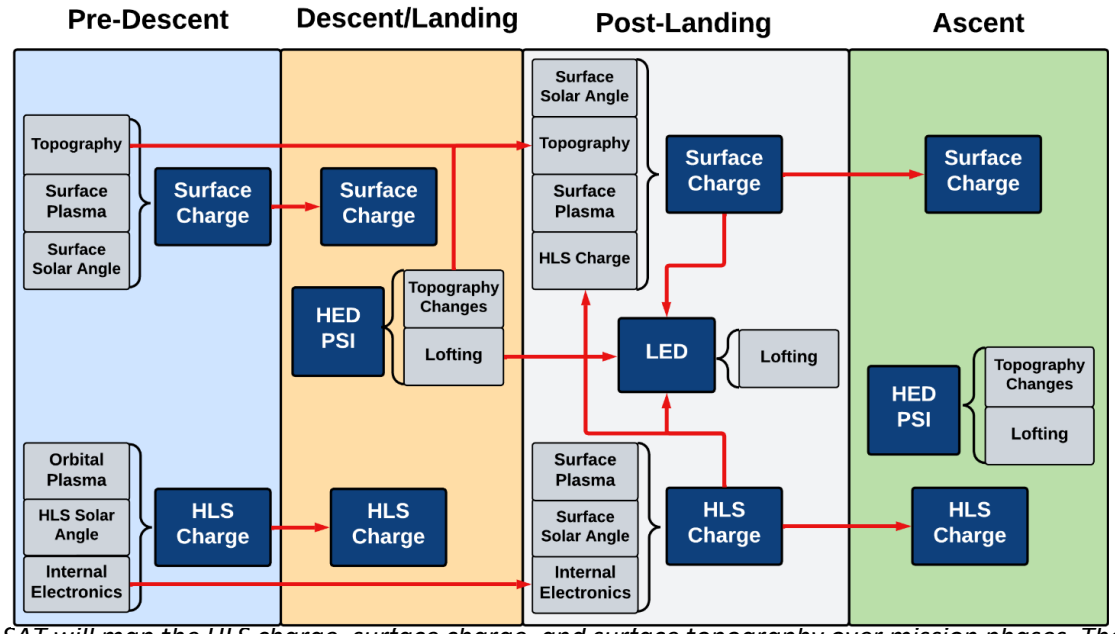

LSAT will map the HLS charge, surface charge, and surface topography over mission phases. The red arrows indicate the inputs and outputs of the various calculations and models.

Key Design Details & Innovations of the Concept

- Step 1: Determine the landing site charge, depending on solar illumination angle and topography
- Step 2: Calculate the charge of the HLS in lunar orbit
- Step 3: Determine dust lofting and cratering (or other topographical changes) from descent and landing operations
- Step 4: Determine the time-varying charge and dust distribution of the landing site and HLS, with the information on the adjusted topography
- Step 5: Assess risks associated with the changing environment
- Innovations: LSAT presents a high-fidelity simulation of the complex lunar surface environment, considering the dynamic presence of the HLS over the entire mission duration. This will be achieved through the construction of a novel framework to integrate several already-existing models.

Summary of Schedule & Costs for the proposed solution's path to adoption

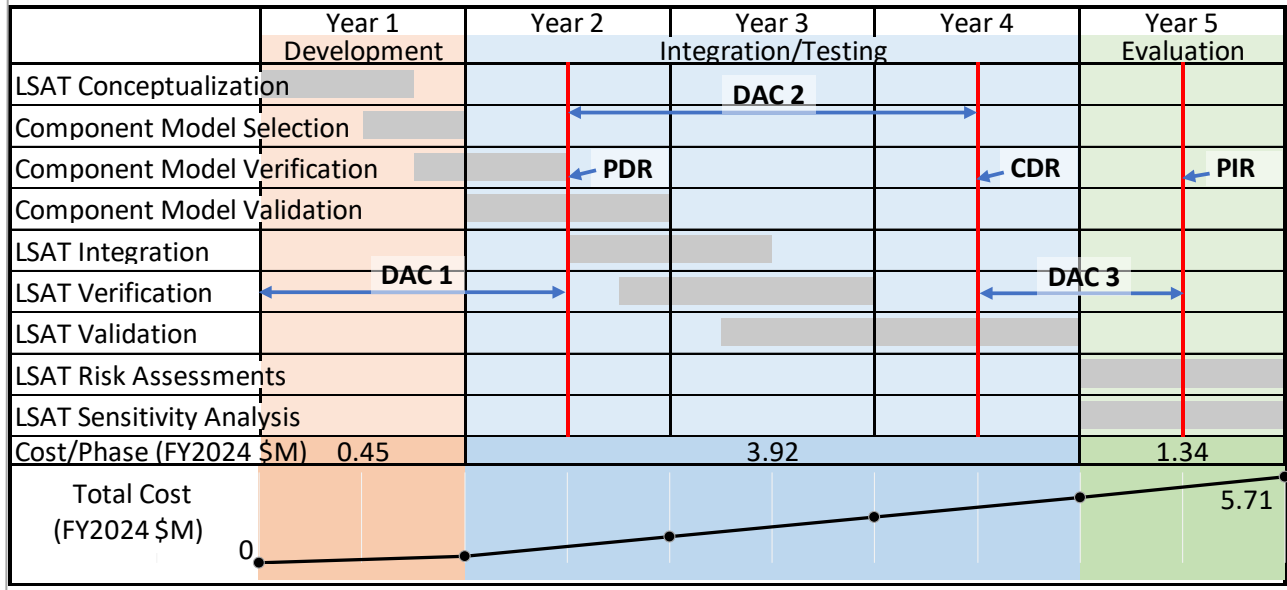

Table of Contents

I. Introduction

Understanding and mitigating the risks posed by the presence of lunar dust is critical to ensure crew and system safety and performance during lunar missions. The lunar surface is exposed directly to deep space, without the protective layer of an atmosphere, resulting in constant exposure to Solar Particle Events, Solar Flares, Galactic Cosmic Radiation, and micrometeoroid impacts [1]. The continuous impact of high energy particles on the lunar surface results in the creation of lunar dust. Lunar dust is traditionally defined as lunar regolith particles with a diameter less than 50 μm [2]. These particles are abrasive and pervasive, having the ability to damage, coat, and adhere to surfaces [3]. Due to the continued exposure of the lunar surface to the deep space environment, the dust may charge to a location-dependent electrostatic potential. The crew on the Apollo missions found that lunar regolith was adhesive, abrasive, and nearly impossible to adequately clean. It was documented in the Apollo 16 mission report that "the dust was always a major cause of concern in that the crew never knew when dust might get into some equipment and compromise the lunar module or extravehicular mobility unit environmental control systems" [4]. The negative effects of dust were not isolated to the Apollo 16 mission. Throughout all six Apollo surface missions, it was reported many systems were rendered inoperable including lunar equipment conveyers [5], suit wrist and hose locks [6], cameras [7], vacuum cleaners [4], extravehicular activity suit (EVA) overvisors [4], sensors [4], and geopallets [8]. System damage was incurred despite design adjustments intended to mitigate dust buildup on components and entry into the habitat. Additionally, dust embedded into crew member's lungs posing a serious health risk [6,9]. Upon descent and landing, dust lofted from the rocket exhaust plume obscured visuals of the lunar surface, adding additional challenges to vehicle landing [10]. High fidelity simulations have been developed to model surface charging and ejecta dynamics; however, a model to assess the risks associated with ejecta over an entire mission duration does not currently exist. The development of a holistic, mission-centric, lunar regolith simulation can be used to assess the potential risks to crew, vehicle, and surface assets over a lunar surface mission.

A. Lunar Surface Environment

To prevent the negative consequences of lunar dust, it is critical to understand the interactions between the natural lunar surface environment and lunar dust to predict the effects on human exploration missions. The Moon's presence within a plasma environment causes the lunar surface to charge to an electrostatic potential. The charging currents that create this electrostatic potential come from four major sources: photoemission of electrons (induced by exposure to solar photons), plasma electrons, plasma ions (both of which are delivered via solar radiation), and secondary electrons (ejected from the lunar surface). The proportions of these four sources of charging currents at the Moon's surface determine the location-specific lunar surface electrostatic potential [11]. As such, the illumination condition at a mission site largely affects the surface electric potential and associated electric fields. There is uncertainty in both the polarity and magnitude of the electrostatic potential. For example, variations caused by the lunar wake, solar wind flow, and Earth's magnetosphere result in changes in the lunar electromagnetic environment [11,12]. Additionally, location specific features, such as magnetic anomalies and lunar topography, have been shown to have effects on uncertainty in electrostatic conditions [12].

The regolith of the Moon's surface is an almost-perfect insulator, enabling location-specific electrostatic potentials [12]. Generally, it is accepted that the lunar dayside charges positively due to the domination of the photoemission of electrons, and that the lunar nightside charges negatively due to the domination of plasma electrons [11,12]. This phenomenon of disparate charge across regions also occurs in Permanently Shadowed Regions (PSRs) near areas of high illumination, such as landing locations. Surface charging has a strong effect on lunar dust dynamics, primarily driving the motion of particles with a diameter of less than 10 μm, which results in the phenomenon of dust lofting. Dust particles may loft due to electrostatic repulsion from the like-charged lunar surface [11]. The lofting height is dependent on the particle size, with 5 μm diameter particles levitating around 10 cm above the lunar surface, and 0.1 μm diameter particles levitating up to 100 km above the lunar surface. Additionally, the location-dependent charge of the lunar surface may induce horizontal electric fields, causing the dust to move across the lunar

surface [12]. The uncertainties present in the electromagnetic characterization of the natural lunar surface environment make lunar dust charging and dynamics difficult to predict, increasing the complexity of mitigating the risks associated with lunar dust. Because of these challenges, Apollo astronaut John Young argued that "Dust is the number one concern in returning to the Moon" [10].

B. Human Landing System Challenges

Our current understanding of the Lunar surface environment is primarily in the context of the natural lunar environment, or an environment which has not been disturbed by human technology or exploration. Future human exploration will disturb the natural lunar environment, making lunar dust dynamics increasingly harder to predict. The lunar surface will be altered through the changes of vehicle electrostatic surface potential in orbit, the exposure of the lunar surface to rocket exhaust plume during descent, changes in lunar topography due to cratering, and a variation in the lofted dust distribution from high velocity ejecta.

The issues and challenges associated with lunar dust are compounded by the presence of a Human Landing System (HLS). Most notably, rocket plume-surface interactions (PSI) have large, but mostly unknown, effects on the lunar environment [13]. The impingement of a supersonic rocket exhaust jet, which the HLS will be using during descent and landing operations, on a granular bed of solid particles causes the particles to disperse with high momentum [14]. During the Apollo program, it was observed that the high-speed particles have the potential to sandblast structures in the landing vehicle's vicinity, causing significant damage to surface assets. Additionally, the lunar regolith may be lofted to altitudes as high as 100m, significantly impacting visibility during landing operations [14]. The hazard created by the high-speed ejecta must be considered thoroughly prior to future lunar missions. The understanding and prediction of PSI enables the ability to minimize surface alterations, mitigate damage to surrounding surface assets, and conduct successful surface exploration. PSI poses numerous risks to crew, mission, and vehicle by degrading visual and sensor performance, decreasing vehicle stability, altering thermal profiles, and damaging the vehicle or surrounding assets via abrasion or high velocity ejecta [10,15].

In addition to PSI, the HLS can alter the lunar environment through changes in electric potential as it moves through different space environments including deep space transit, cislunar orbit, and the lunar surface [16]. This alters the electric potential and subsequent modeling parameters of lunar dust. In transit to the Moon as well as in cislunar orbit, active electrical avionic components within the HLS and the exposure to the lunar orbital plasma environment will charge the conductive spacecraft surface prior to approaching the lunar surface [17]. After landing, the charge associated with the spacecraft surface will change, as the lunar orbit plasma environment is unique from the lunar surface plasma environment [18]. However, just as the plasma environment will affect the charge on the HLS, the presence of the charged HLS will affect the lunar surface electric potential environment. These changes have implications on the performance of solar panels, thermal systems, sensors, and EVA operations. Furthermore, the lander plumes, which will be activated during descent, landing, and ascent, will affect lunar topography and induce dust lofting [19].

Apollo missions provided initial insight into the risk and effects of rocket PSI but cannot be strictly extrapolated for future HLS due to potential differences in engine configuration and landing location. Therefore, improved modeling techniques need to be implemented to increase the understanding of these highly complex, dynamic systems. Additionally, it has been shown that electrostatic charges have significant effects on dust lofting and settle time, posing risks to EVA operations [3]. The incorporation of the changes in electrical potential throughout a lunar surface mission needs to be incorporated into these modeling systems to adequately capture surface changes and quantify mission risks.

Overall, the lunar surface environment coupled with the HLS is challenging to understand and predict. However, lunar dust dynamics must be determined to mitigate risks to crew health, system performance, and mission success. We propose the development of the Lunar Surface Assessment Tool (LSAT): a holistic, mission-specific lunar surface simulation that evaluates the effects of topography, illumination conditions, mission timing, HLS landing operations, and HLS surface charge on lunar surface charge and associated dust dynamics.

II. Solution Description

While high fidelity simulations of astrodynamics, lunar surface charging, and PSIs exist, the combination of these simulations into a holistic mission-centric model has not yet been achieved. By leveraging available models, we can create a flexible simulation for lunar surface missions that considers various landing locations, engine configurations, and epochs. LSAT enables us to perform a trade study on these factors from a lunar dust risk perspective, informing mission and system design. Many of the components that would comprise LSAT have already undergone initial verification and validation, resulting in a TRL range of 3-9 [19–21]; therefore, LSAT development and associated verification and validation can begin immediately. We plan for this model to be implemented in the early stages of mission planning in order to perform necessary trade studies for identifying the technology and research imperative to lunar dust risk mitigation. As such, this technology is inherently low risk and enables the further decrease of lunar surface exploration risks. Leveraging already-existing models enables the creation of LSAT within 3-5 years, allowing for the use of this tool in upcoming lunar missions.

LSAT, a physics-based dust dynamics prediction tool, addresses the PSI Modeling and Validation category of the Human Lander Challenge (HuLC). LSAT enables the assessment of the risks associated with lunar dust and subsequent mission risk mitigation. NASA's Plan for Sustained Lunar Exploration and Development notes that the Artemis Base Camp will be located at the lunar south pole, where the proximity of PSRs to illuminated landing areas enables the investigation of volatile compounds [22]. As such, particular attention will be paid to the illumination conditions associated with the topographies of the published candidate landing sites to determine the local electric fields. The NASA CrossProgram Design Specification for Natural Environments (DSNE) notes that the lunar surface geological and geomorphological environments affect all space systems. Therefore, it is required to be considered for all surface system design. As such, they suggest that "individual landing site data should guide mission planning" [23]. By utilizing Digital Elevation Models (DEM) generated by the Lunar Orbiter Laser Altimeter (LOLA) [24], we will directly address specific landing sites. Furthermore, our consideration of the various currents for lunar surface charging, lunar regolith particle size distribution, morphology, and chemical composition will be enabled by the DSNE's lunar surface environmental specifications.

A. Modeling Methodology

LSAT will first determine the electric fields and potentials of the candidate site prior to HLS landing. The astrodynamics model will provide the solar illumination angle at the latitude/longitude of the candidate site, while LOLA data will provide a DEM to enable construction of a dielectric lunar surface within the charging model. This charging model will also be used to determine the charging of the HLS when in lunar orbit, prior to descent. The high-energy dynamics PSI (HED PSI) model will be used to determine the PSIs, including the lofted dust from descent and landing, cratering, and topography changes. A new HLS charge that incorporates the ion flow from the thrust chamber to the exhaust during landing operations will be calculated using an equilibrium chemistry model. The topography changes and HLS charge will be used within the charging model to iteratively calculate the new electric fields and potentials over time. The lofted dust will be assumed to be initially at a charge identical to that of the surface prior to descent. Settling time will be calculated based on lofted dust particle size distribution, charge, and the time-varying charge of the lunar surface by using a low-energy dynamics (LED) model. The HED PSI model will be used to determine the PSIs during ascent and evaluate the topographic changes during that phase. This methodology is depicted in Figure 1.

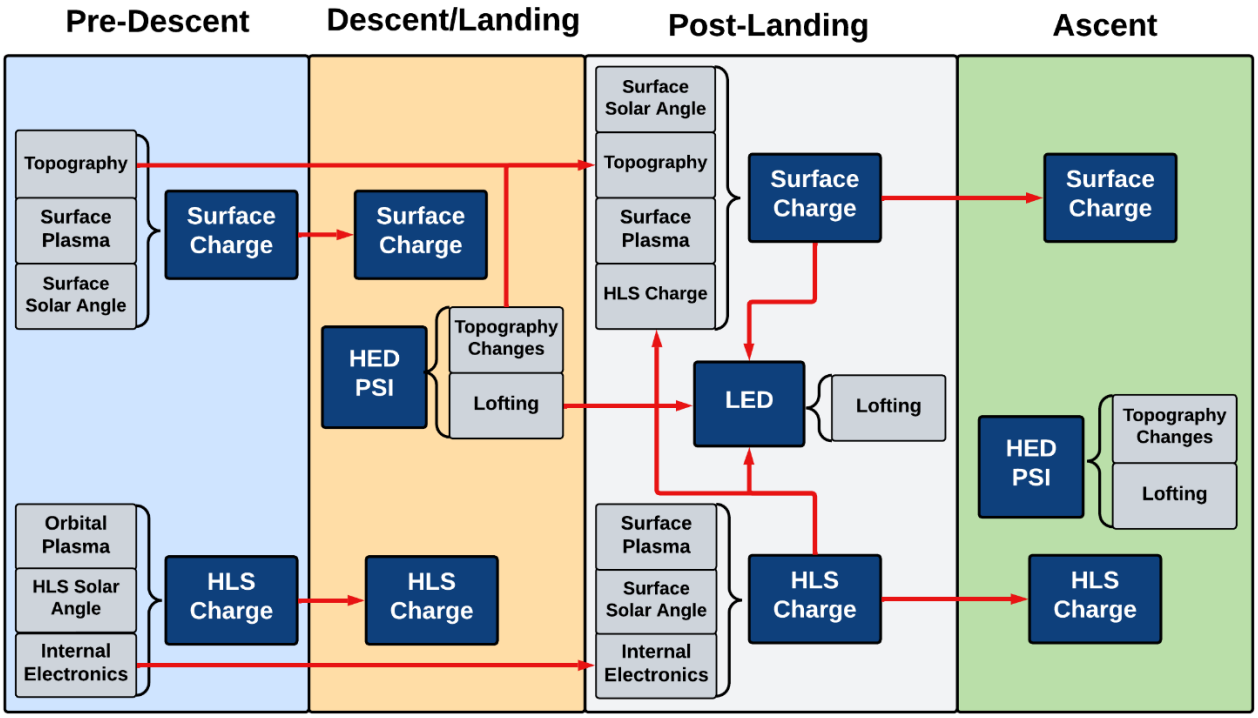

Figure 1. *LSAT Methodology. LSAT will map the surface charge and HLS charge across various mission phases, informed by surface and orbit plasma environments, topography, solar illumination angle, and PSI models. The red arrows indicate how information feeds between the models, across the various phases. HED PSI refers to a model for high energy dust dynamics, as created by plume-surface interactions. LED refers to a model for low energy dust dynamics, such as settling time.*

Figure 1 indicates the in-depth transfer of information across the mission phases. In the Pre-Descent phase, the initial surface topography, surface plasma environment, and solar angle at the surface are used to determine the spatially varying lunar surface charge. Similarly, the orbital plasma environment, the solar angle at the HLS, and the HLS internal electronics are used to determine the charge on the surface of the HLS. In the Descent/Landing phase, the lunar surface charge and HLS charge are initialized based on the surface charge and HLS charge calculated in the Pre-Descent phase. A HED PSI model is used to calculate the topographical changes and dust lofting spatial distribution based on the thruster configuration and the high-energy dynamics associated with the sandblasting of the lunar regolith. Next, in the Post-Landing phase, the topographical changes associated with the Descent/Landing phase are incorporated with the initial topography in the Pre-Descent phase to generate a new surface topography. The lunar surface charge is determined based on the solar angle at the surface, the new topography, the surface plasma environment, and the HLS charge. The HLS charge is determined by the surface plasma environment, the solar angle at the surface, and the internal electronics. The dynamics of the dust that was lofted during Descent/Landing is determined using a LED model, which considers the lofted dust (as determined in the Descent/Landing phase), the HLS charge, and the lunar surface charge. Finally, in the ascent phase, the lunar surface charge and HLS charge are initialized as the charges associated with the end of the Post-Landing phase. Similarly to the Descent/Landing phase, a HED PSI model will be used to calculate the topography changes and dust lofting associated with thruster firing.

As shown in Figure 1, the modeling elements of LSAT are grouped into surface charge, HLS charge, HED PSI, and LED. An additional modeling element, solar angle, is an input to both the surface charge and HLS charge models. An external model, or group of external models, were chosen to represent each of these

elements on the following criteria: derivation of results from a first-principles analysis and rigorous validation.

B. Component Model Selection

LSAT is the holistic integration of critical lunar surface models incorporating lunar surface electrostatic potential, topography, illumination conditions, mission epoch, and HLS charging. As such, LSAT uses preexisting, validated models. Spacecraft, Planet, Instrument, C-matrix, Events information system (SPICE) is used to simulate the astrodynamics of the Moon-Sun-Earth system to generate the solar angle and the position of the Moon within Earth's magnetosphere at specific mission times. SPICE was developed by the Navigation and Ancillary Information Facility (NAIF) and has been used in a variety of NASA missions including Cassini, the Mars Exploration Rover, the Mars Reconnaissance Orbiter, and DAWN [21]. SPICE will be used to generate the solar angle on the lunar surface. This lunar parameter will then be fed into Spacecraft Plasma Interaction Software (SPIS) to calculate the electric environment associated with the combination of lunar topographical features, the lunar plasma environment, and the HLS.

SPIS will be used to simulate surface charging of both the topographically complex lunar surface and the spacecraft surface. As such, it is the primary model for both the lunar surface charge and HLS charge aspects of LSAT. SPIS was developed by a consortium led by ONERA and uses a particle-in-cell (PIC) modeling approach with a non-linear form of the Poisson equation solver to calculate the electric field over volumes and surfaces represented by an unstructured mesh [17,20]. SPIS uses a combination of Dirichlet and Robin (Dirichlet-Neumann combined) boundary conditions to simulate sheath or pre-sheath conditions [20]. The structure placed within the plasma environment calls upon a comprehensive list of material properties, including secondary emission, conductivity, field emission, and sputtering. The internal spacecraft electronics can be modeled through an equivalent circuit [20]. Validation of this tool will be achieved through a separate, first-principles analysis of the surface charging associated with simple geometries (sphere, cylinder, etc.) in various plasma environments. Drawing from Hilgers et al. (2008), the implementation and comparison of data generated via Langmuir probe models will greatly assist in validating SPIS for implementation in lunar surface environments [17]. Overall, the combination of these elements renders SPIS a powerful tool to use for an initial analysis of the electromagnetic environment created by the combination of lunar plasma, lunar topography, and an active spacecraft.

For HED PSI modeling, the NASA-proposed combination of Gas-Granular Flow Solver (GGFS), Loci/CHEM Computational Fluid Dynamics (CFD) Program, and the Debris Transport Analysis (DTA) post-processing tool will simulate cratering and lofting during descent/landing and ascent. GGFS, developed by the CFD Research Corporation (CFDRC) and the University of Florida, is a high-fidelity granular phase particle physics model that enables the prediction of the liberation and flow of regolith under "extreme environments," such as the lunar surface that is affected by a supersonic and partially-rarefied rocket exhaust flow [25]. This simulation program allows for both Eulerian-Eulerian and Lagrangian Discrete Element Modeling (DEM) approaches. The former may be used to simulate erosion, cratering, and transport, while the latter may be used to calculate granular particle interactions for complex morphologies [25]. The Loci/CHEM flow solver simulates three-dimensional flows of chemically reacting mixtures of gases. This solver enables the calculation of multi-component mixing with consideration for complex geometries and object motion. This solver is often used by the Fluid Dynamics Branch at Marshall Space Flight Center (MSFC) and has been thoroughly verified [26]. The DTA framework was initially developed to analyze the STS-107 accident, during which the wing of the Space Shuttle Columbia was struck by foam debris during ascent, resulting detachment during re-entry [27]. The DTA simulation has been shown to be capable of performing transient debris transport simulations, tracing the debris trajectories through a time-varying flow simulation such as the ascent of a launch vehicle or the propulsive descent of a lander [27].

The high-fidelity CFD simulations of the fluid flow features that may transport debris include rocket plume entrainment and impingement, which may be used to simulate plume effects on lunar regolith. The combination of Loci/CHEM and the DTA simulation framework has been used by the MSFC Fluid Dynamics Branch in analyzing Mars lander debris transport. The incorporation of GGFS will enable the calculation of topography changes and lofted dust for the purpose of a more thorough assessment of the risks to exploration systems and EVA activities. The full integrated simulation framework including GGFS, Loci/CHEM CFD, and DTA have been fully implemented on NASA supercomputers and have demonstrated 2-dimenstional simulations, thus showing operationality [25].

The last modeling element of LSAT is a patched charge model that simulates LED during the post-landing phase. Calculation of low-energy dust dynamics requires the consideration of elements such as dust grain morphology, grain size, charge, grain initial velocity and position (determined from the method of lofting, such as EVA movement or landing operations), and plasma environment. Wang et al. (2016) developed a patched charge model to study the interactions between dust particles on a dusty surface [28]. In this model, dust particles are no longer assumed to have a single charge, but rather have different charges on different portions of their surface area, depending on the environment. The formation of microcavities between neighboring dust particles on a dusty surface may lead to a repulsive electrostatic force that is adequate to spontaneously loft a particle above the dusty surface. Further work on this model by Carroll et al. (2020) considered varying morphologies, finding a relationship between particle shape and "launch velocity", which is the velocity by which a particle is lofted from a dusty surface [29]. Yeo et al. (2021) used the patched charge model to study the dynamics of lofted dust, considering grain photoemission, grain secondary electron emission, electron collection currents from the photoelectron sheath and solar wind, and the solar wind ion current [30]. Dust grain size was varied in this work, and the particle irregular morphology was simulated using the relationship between particle launch velocity and shape determined by Carroll et al. (2020). Overall, this model is promising for the study of LED at the lunar surface, with some adjustments to enable the simulation of already-lofted particles.

C. Component Model Verification and Validation

LSAT validation will occur in several steps. First, the combination of SPICE and SPIS will be validated through a comparison to Lunar Prospector Electron Reflectometer data [11]. As the Lunar Prospector charged to some potential, SPIS will be used to determine the charge of the spacecraft surface in the lunar orbital plasma environment, using an equivalent circuit to simulate the electrical field generated by the spacecraft electronics. Then, the topographies of the lunar dayside and nightside will be imported into SPIS, while the illumination angle associated with these locations over the epochs of data collection will be calculated using SPICE. SPIS will be used to determine the fundamental electric potential at these locations. The comparison of the spacecraft charge to the analytical calculations communicated in Stubbs et al. (2008), combined with the collected data by the Electron Reflectometer will provide us with an evaluation of the efficacy of SPICE and SPIS to predict lunar regolith charging and spacecraft charging. Next, the SPIS model will be used to determine the charge of the spacecraft through the various regimes: lunar orbit, descent, landing, and ascent. This simulation will be validated through a simplified first principles analysis which uses information about the plasma environment on the lunar dayside.

D. Experimental Verification and Validation

The HED and LED models will be combined with SPICE and SPIS to create LSAT, which will be experimentally validated. There are two primary goals for the planned experiments: validate the HED model, with a specific focus on sandblasting and topographic changes, and validate the LED model, with a specific focus on lofting and 3-dimensional particle size distribution. These experiments will be performed in a large Thermal Vacuum Chamber (TVAC) lunar-analogous environment. An example chamber that may be used is the Glenn Research Center (GRC) "Dirty" Vacuum Chamber [31]. Various lunar regolith

simulants (e.g., JSC-1A, Exolith Lunar Mare Dust Simulant, Lunar Highlands Simulant) that represent different topographical regions of the lunar surface will be placed within the vacuum chamber. For HED model validation, the full range of particle sizes included in the simulants will be used. For LED model validation, the simulants will be baked out (to ensure no humidity-based clumping is present) and sieved to constrain the maximum particle size. A solid surface, simulating the bedrock, will be placed under a layer of dust of known thickness. An ion thruster will be used to charge the dust and generate a lunar surface-analogous plasma environment [32], which can be characterized with Langmuir probes and simulated within LSAT. A simplified geometry "spacecraft" will be charged to an electric potential associated with the lunar orbital environment. The spacecraft will descend onto the regolith, using cold nitrogen gas to represent the forces associated with the thruster plume. The thruster firing will induce HED, resulting in a distribution of dust particle sizes and velocities throughout the chamber, altered by the initial charge associated with the dust and the constructed plasma environment. The dust particles will slowly settle within the chamber, driven by LED. High speed cameras will be used to analyze the HED and LED associated with particles of various masses, morphologies, and initial charge/positioning. Particle tracking software will be used to track the trajectories of lofted particles, while the particle size will be used to determine the mass. This information will be used to determine the trajectory as a function of particle mass and initial position in the test chamber.

Several test cases will be used to validate LSAT. The dust will be charged to a range of electric potentials, from -4000V to 20V. These values were derived from Lunar Prospector measurements of the electrostatic charge of the lunar surface in various solar activity, geomagnetosphere positioning, and illumination conditions [33]. A UV lamp, analogous to the sun, will be placed within the vacuum chamber at various positions, enabling the experimental simulation of illumination conditions and associated charging. During the thruster firing, the motion of the dust particles will be monitored to determine a relationship between the initial charge of the dust and the trajectory shape. These trajectories, combined with information on the moving particle size distribution, will be compared to LSAT-generated data. Additionally, the trajectory of the particles, associated proximity of the particles to the "lander," and charge associated with the dust particles and the conductive lander surface, will be used to assess the risk of arcing. This assessment will continue after "landing" to determine the change in arcing risk over time. LSAT will be used to replicate the experimental setup to compare the computational results to experimental results of the charge and particle distribution. This experimental setup has utility in providing experimental data for LSAT validation but also contributes to our greater understanding of PSI regardless of the implementation of LSAT. Past work has explored cratering and particle ejecta tracking in a large scale vacuum chamber but did not incorporate electrostatics into the testing conditions [42]. The proposed experimental design builds upon this past work to not only provide but a method to validate the HED and LED elements of LSAT, but also increase our fundamental understanding of ejecta dynamics in a charged environment [42].

E. LSAT Assumptions

The assumptions associated with LSAT comprise those included in the individual component models. We are assuming that the lunar topography of the candidate landing sites is simple enough to model adequately in SPIS, the spacecraft surface conductivity is constant across all areas of the spacecraft, , and the spacecraft internal electronics can be represented by an equivalent circuit. The PSI model assumes that the ground is adequately flat, negating the need for complex topography modeling, and that the lunar bedrock does not impede cratering. The engine configuration will be initially assumed to be identical to that for an Apollo era lunar module due to the existing data and PSI models on this vehicle type. After verification and validation of LSAT for the Apollo era lunar module are achieved, the engine configuration for the HLS will be updated to more recent landers, such as Intuitive Machines Liquid Methane & Liquid Oxygen engine on the IM-1 Nova-C class lunar lander [34]. To evaluate maximum EVA risk, non-collision

conditions (particle-particle or particle-spacecraft) will be assumed to maximize particle settling time and particle upward velocity. For all models, we assume conservation of mass, momentum, and energy.

F. Integration Feasibility Assessment

It should be noted that the integration of the astrodynamics, surface charging, HED, and LED models into a single simulation is challenging. Parameters associated with the individual models, such as time steps and the spatial domain, must be assessed and synchronized to enable seamless model patchworking. Therefore, prior to the choice of individual models, the ability of models to be integrated must be thoroughly assessed via a parameter analysis. To evaluate the integrability of the models described in Section II.B: Component Model Selection, the combination of SPICE, SPIS, and LOLA topographic data was assessed.

First, First, LOLA data for Haworth Crater was used to create a topographic surface in MATLAB, as seen in Figure 2a [24]. This surface spans an area of 29,800 m x 29,800 m, with a resolution of 25 m^2 (5 m/pixel). This is the maximum resolution that can be achieved with the given data set. The uncertainty of this data is 10-20 cm horizontal and 2-4 cm vertical [35]. While a greater resolution is desirable to accurately integrate the HLS and descent/landing topographical effects in this model, we determined that this resolution is adequate for an initial integrability assessment.

Next, SPICE was used to calculate the azimuth and elevation angles of the Sun with respect to Haworth Crater's latitude and longitude. SPICE allows for a calculation of these angles every second; however, it was determined that this resolution was unnecessary for this initial test. Instead, the azimuth and elevation angle were calculated every 24 hours at midnight to visualize how the changing Sun angle affects illumination conditions at this candidate landing site [36]. This visualization of illumination may also be used to inform the selection of a specific landing location within the 29,800 m x 29,800 m section of Haworth crater that was simulated. Additionally, the shadows associated with the topographically diverse South Pole landing sites make navigation and landing challenging for both autonomous landing systems and pilots. While future lunar missions will have Lunar Reconnaissance Orbiter (LRO) topographic maps available for navigation, the time-varying illumination visualization may be used to help train guidance systems and crew [37]. Figure 2b displays the Haworth Crater simulated surface on midnight June 7, 2025 and midnight June 14, 2025. Based on the Sun angle, various features of Haworth crater are either lit or shadowed. In the one week difference simulated, the illumination profile of this landing location changes dramatically. Therefore, illumination considerations are critical for a holistic, high-fidelity simulation of lunar missions.

(a)

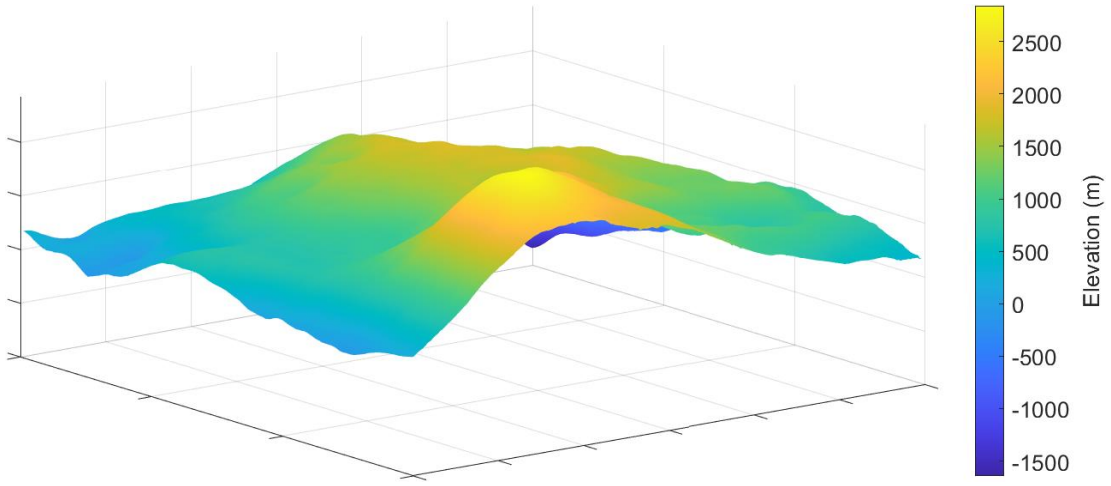

(b)

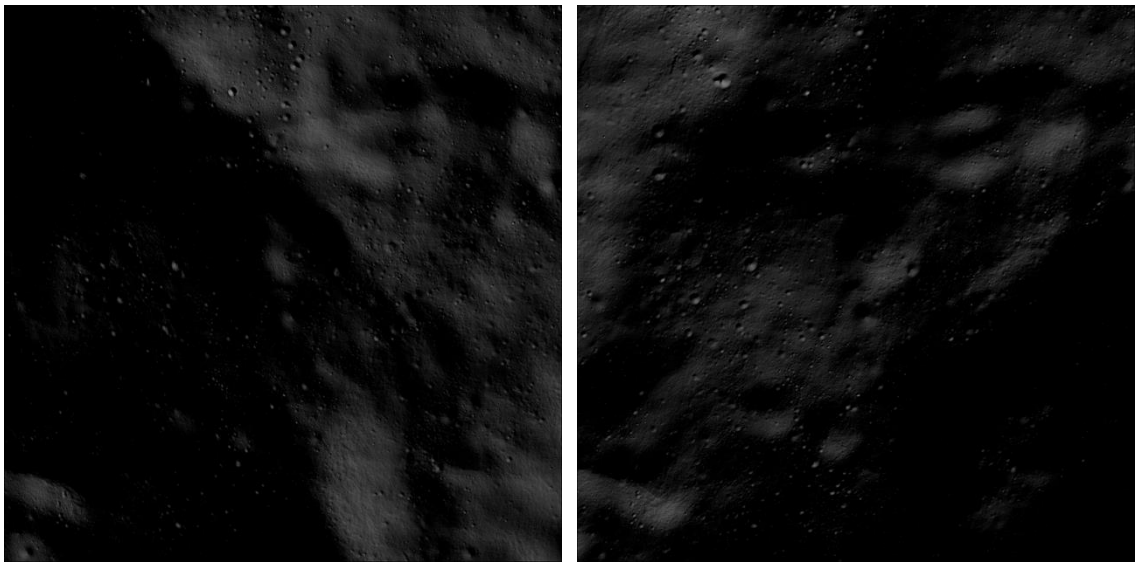

June 7, 2025 June 14, 2025

Figure 2. *Haworth Crater Topography and Illumination. (a) Construction of Haworth Crater lunar topography from LOLA data. (b) Calculation of solar illumination angle in SPICE and associated shadowing on the Haworth Crater lunar topography. As the solar illumination angle changes, so do the shadows.*

Next, the ability of SPIS to model the lunar surface, plasma environment, and HLS was assessed. A cloud of points that represented the Haworth Crater surface was imported into SPIS, and then tessellated to create a surface mesh. The tessellation triangle size may be altered based on the desired mesh resolution; however, decreased triangle size for increased resolution greatly increases computational time. Therefore, when integrating SPIS with topographic data, the minimum adequate resolution should be used. The construction of the Haworth Crater 29,800 m x 29,800 m section is shown in Figure 3a.

The HLS, assumed initially to be a similar size to the SpaceX starship vehicle [38], was simulated both in the deep space environment and on the lunar surface. The construction of the deep space environment simulation in SPIS is shown in Figure 3b. The HLS is placed in a computational volume with an associated computational boundary. The qualities of the plamsa that fills this computational volume can be set within SPIS. This modeling tool provides standard plasma environments associated with high or low solar activity, along with plasma environments associated with the Earth's magnetosphere. The construction of the landed HLS simulation in SPIS is shown in Figure 3c. To shorten simulation time, a 1000 m x 1000 m section of the Haworth Crater topography was selected for modeling. Within SPIS, the HLS was loaded into the simulation space about 1000 m above the surface. The smallest distance between the landing vehicle and the surface directly below it in the -Z direction was calculated to translate the landing vehicle to the surface, using the built-in "Land S/C" feature in SPIS. Future steps involve merging the mesh of the landing vehicle and the surface to enable a 3-dimensional mesh creation, which may be used for the necessary subsequent computational steps and the calculation of surface charging. The plasma environment associated with the lunar surface may be simulated using the built-in plasma environments associated with SPIS.

(a)

(b)

(c)

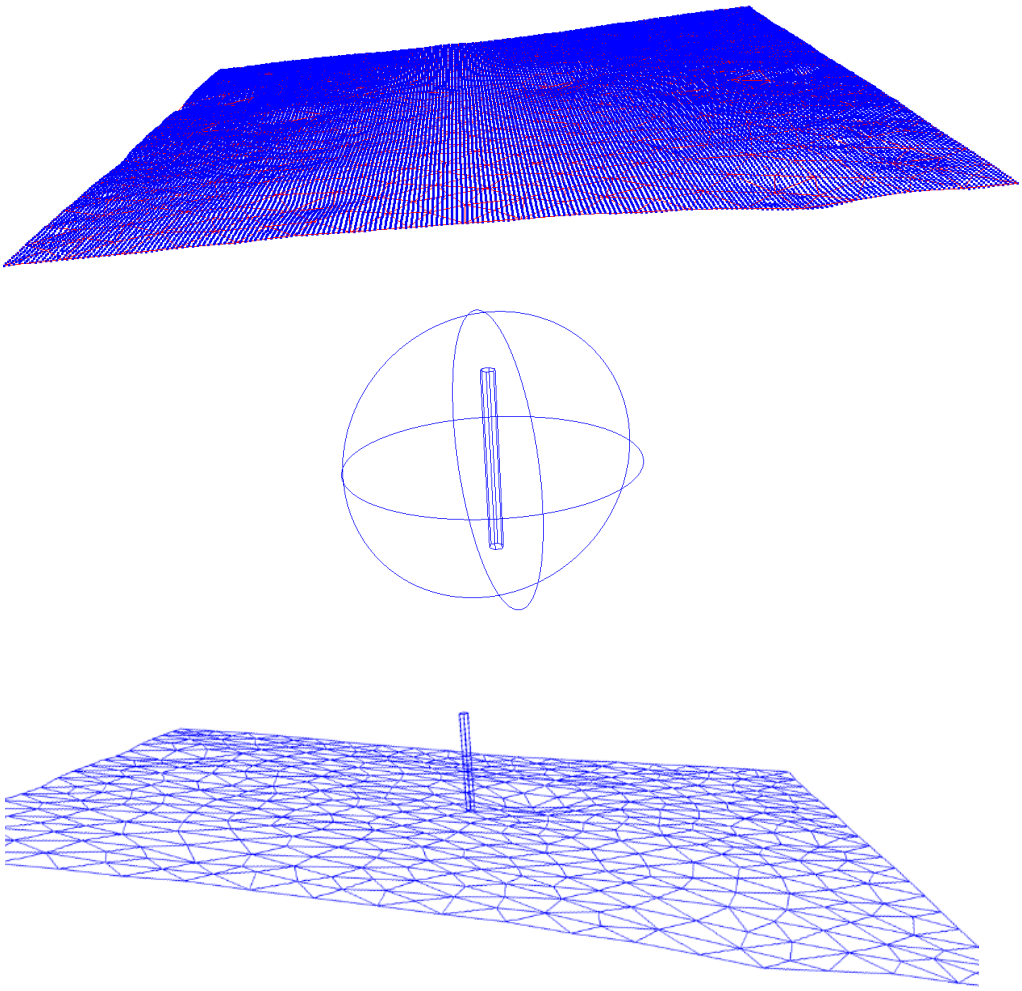

Figure 3. *LSAT Integration Feasibility Assessment Steps. (a) Import of lunar topography into SPIS and construction of a tessellated simulation mesh. (b) Starship-sized HLS and associated spherical computational volume for deep-space charging simulations in SPIS. (c) Simulation set-up for a landed HLS on a section of Haworth Crater.*

III. Solution Value: Risk Assessment and Quantification

Through the combination of charge models, HED models, and LED models, LSAT will enable a thorough risk assessment and quantification to inform mission logistics planning for lunar surface missions. The outputs from the models will be used to perform a risk analysis that evaluates identified risks to estimate likelihood of occurrence, consequence of occurrence, and timeframe for necessary mitigation actions. Risk quantification results will be focused on LSAT outputs, which have the most significant effect on the risk to EVA including crew safety and mission success. Sensitivity analysis of risk models can be used to identify the most significant factors and aid in the development of priorities for risk mitigation. Because of the complexity of multiphase flow systems, a non-intrusive uncertainty quantification (UQ) based approach is recommended to identify the most influential parameters in each case. Optimal parameters for analysis may be determined in future work through methods such as deterministic or Bayesian calibration. The open-source software Nodeworks developed by National Energy Technology Laboratory (NETL) will be used for the sensitivity analysis. Nodeworks is a graphical interface designed to create surrogate models to

represent complex computational science and engineering models where direct analysis is too computationally expensive. From these surrogate models' optimization, sensitivity analysis, uncertainty quantification, and deterministic calibration can be done [39]. Ultimately, the goal of a sensitivity analysis would be to identify trends in illumination, topography, and plasma environment parameters that indicate an increased risk of degraded crew and system health and performance. Additionally, LSAT can be used to assess the time-dependent likelihood and consequences of the risks associated with ejecta, providing a dynamic analysis of these risks over the mission duration.

Outputs from modeling efforts, including risk analysis and assessment of parameter sensitivity, can be used to inform trade study variables, weights, and criteria for landing site location. Currently there are 13 proposed areas of scientific interest for the Artemis program near the South Pole, selected for proximity to PSRs, continuous access to sunlight for a 6.5 day period, terrain slope, and ease of Earth communications [40]. While these evaluation criteria are adequate for an initial selection for candidate mission sites, further analysis must be performed to understand the effects of the HLS on the mission sites. Site-specific parameters such as regolith material type, regolith particle size profile, and regolith electrostatic potential must be considered. Additionally, HLS-varied parameters such as topography, illumination profile, sand-blasted ejecta size/position, HLS electrostatic potential, and lofted dust dynamics/settling time (dependent on sand-blasted ejecta profiles and the regolith and HLS charges) must be analyzed to thoroughly understand the risks associated with specific mission sites. LSAT model outputs will enable the following evaluation criteria to be used to perform a landing location trade study: lofted dust size distribution, lofted dust settling time, lunar topographic changes, damage to vehicle from ejecta, electrostatic potential, and arcing risk. A further description of these evaluation criteria is included in Table 1. As EVA will be critical for upcoming lunar missions (i.e. moonwalks to PSRs for Artemis III science objectives) [37], the stated evaluation criteria were specifically selected for consideration of EVA risk. Other evaluation criteria may be considered for different mission profiles or scope. While the sensitivity analysis may provide initial information on weighting of each criterion, additional consideration may depend on mission specific operations such as proximity to areas of scientific interest, EVA scheduling, or presence of surface assets.

Table *1*: PSI evaluation criteria for lunar landing location considering risk to surface EVA operations.

Evaluation Criteria	Reasoning
Lofted dust size distribution	Lofted dust risks include material abrasion, entry into eyes or lungs of crew members, and system performance degradation. Each of these risks may be associated with a specific size range of the lofted dust.
Loft dust settling time	Due to the lack of an atmosphere, reduced gravity, and the lunar plasma environment, dust settling times may affect EVA missions long after vehicle landing.
Topographic changes	Cratering and erosion from HLS rocket plume may result in significant changes to local topography altering EVA missions and changing electrostatic potentials.
Vehicle ejecta damage	Informed by DTA impact analysis, relative kinetic energy, velocity, and impact angles of the debris particle may result in risk to the vehicle.
Electrostatic potential	Electrostatic potential between the vehicle, lunar surface, and astronauts may pose a threat to crew safety and inform the development of grounding technology.
Arcing risk	Dust lofted during descent may pose a risk to crew members by increasing the risk of arcing.

There are risks associated with the adoption of LSAT in mission logistics planning. Inadequate verification and validation of the model may result in inaccurate risk assessments and the support of logistical decisions that result in harm to the mission, vehicle, or crew. Verification factors such as software quality assurance, first principles calculations, and user error can be used to increase credibility in the model and decrease the risk of an adverse outcome. Decreasing the risks associated with validation can be more challenging, due to the small volume of relevant experimental data to validate LSAT against. Often PSI or solid-solid collision models are validated against other models in the literature, which could result in unintended error propagation. The risk of inadequate model validation can be mitigated through performing our own experiments to generate data for model comparison. Additionally, the use of LSAT may be used in a manner to bound the risk limits of a system. For example, the upper bounds for lofted regolith exposure and particle density can be determined to inform requirements for EVAs or surface assets. Moreover, lower bounds may be defined for quantified vehicle risk, as the bulk projected flight path of particles may deviate away from the vehicle due to the non-collision assumption discussed in Section II.E: LSAT Assumptions. In this way, outputs from LSAT can be used while the associated risk is decreased.

IV. Project Schedule and Milestones

A. Budget

Determination of the budget associated with ground software design/development was primarily achieved by using the NASA Project Cost Estimating Capability (PCEC) [41]. This parametric tool enables the calculation of several mission types and subsystems. By using the built-in Work Breakdown Structure (WBS) template for ground software, the cost of the development of ~10,000 lines of code were determined. This value is a conservative estimate, and we expect the actual number of lines of code to be significantly lower. Cost associated with procurement of individual component models was not considered, as the various component models studied in this proposal are open-source and free-for-use. Table presents a breakdown of the software development and experimental costs associated with the LSAT. A margin of 30% was used to account for unforeseen costs (software costs, additional experiments, etc.). An estimated percentage was used to allocate budget to the Development (10%), Integration & Test (60%), and Evaluation (30%) phases, determined through an analysis of the goals and deliverables associated with these phases. Cost of the experimental validation of LSAT can be seen in Table .

Table 2: LSAT Experimental Validation Costs

Item	Quantity	Cost/Unit	Total Cost	Vendor
Ion Thruster	1	$10,000	$10,000	N/A (custom)
Ion Thruster Labor		$15,000	$15,000	
UV Lamp	1	$2000	$2000	
VF-13 Vacuum Chamber	N/A	$460,000	$460,000	NASA Glenn Research Center
Langmuir Probe	3	$1000	$3000	N/A (custom)
Langmuir Probe Labor	3	$1500	$4500	
DC Power Supply	2	$1100	$2200	Keysight
FLIR Camera	3	$1200	$3600	FLIR
VEO 710L Camera	1	$150,000	$150,000	Phantom
V2511 High-Speed Camera	1	$150,000	$150,000	Phantom
TMX 7510 Ultra High-Speed Camera	1	$150,000	$150,000	Phantom
PD-MX motor	1	$400	$400	PDMOVIE

PDL-SCC Universal Thumb Wheel Focus	1	$200	$200	PDMOVIE
LED Lamp (1000 W)	1	$500	$500	HSVision
DC LED Lamp (50 W)	2	$40	$40	Lysed
Liquid Nitrogen			$250	
LMS 1-D Lunar Mare Simulant	3	$65	$195	Exolith
LMS 1-D Lunar Highlands Simulant	3	$65	$195	Exolith
Sieve	2	$250	$500	Cole-Parmer
Safety (gloves, glasses, etc.)			$200	
Total			**$952,780**	

The materials reported in Table 2 were primarily derived from the experimental setup reported by Rubio et al., (2021). These include the cameras, motor, remote focus, and LED lamps [42]. The cost associated with the use of the VF-13 Vacuum Chamber was determined based on discussions with the Facility Manager of the chamber, accounting for 5 experiments performed over 5 weeks, assuming that each experiment must be built-up and torn-down individually and the chamber must be fully cleaned between experiments. The N/A (custom) values are logical estimations; however, these values are subject to change as the necessary fidelity and methodology of the experimental work is determined. The labor costs associated with custom materials were estimated to be 150% of the materials cost; however, the actual costs associated with labor will depend on the complexity of the component and may be much higher or lower than the estimated value presented. The total cost associated with experiments is included in the Integration & Test phase of LSAT development.

Table 3: Costs Associated with LSAT Development, Integration & Testing, and Evaluation (FY2024 $M).

	Development	Integration & Test	Evaluation
Software Development	0.34	2.06	1.03
Experiments	-	0.95	-
Total (no margin)	0.34	3.02	1.03
Total (with margin)	0.45	3.92	1.34

With cost consideration for software development, experimental work, and a 30% margin, the total cost associated with LSAT is $5,710,000.

B. Timeline

LSAT development will occur over five years. The first year will be spent finalizing the Development phase, in which the conceptualization of LSAT and the component model selection will be finalized. Component model verification and validation initiate the Integration/Testing phase, which occurs in years 2-4 to integrate, verify, and validate LSAT. Finally, the Evaluation phase consists of the risk assessments and sensitivity analysis, performed in year 5. Several milestones will ensure adequate project progression: Design Analysis Cycle (DAC) 1 concludes in a Preliminary Design Review (PDR) at year 1.5, which initiates DAC 2. DAC 2 concludes in a Critical Design Review (CDR) at year 3.5. DAC 3 concludes at the Program Implementation Review (PIR) at year 4.5. A pictorial depiction of this schedule, integrated with the costs associated with each phase and the total cost over the five-year period, can be found in Figure 4.

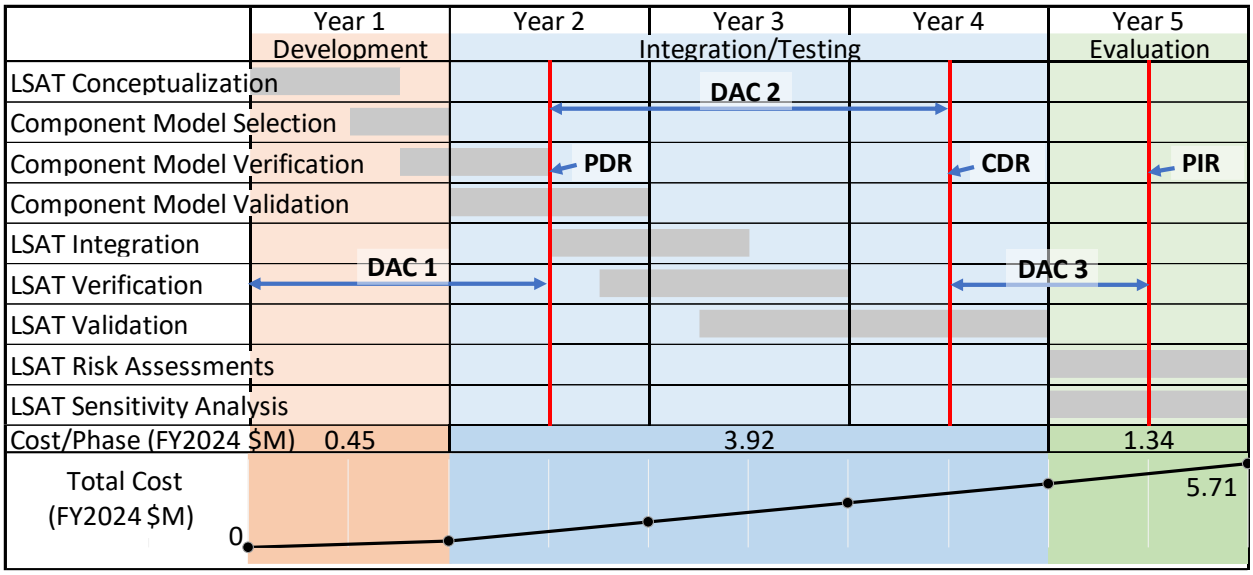

Figure 4. *LSAT Timeline. LSAT development is estimated to take a maximum of five years, consisting of Development, Testing, and Evaluation phases.*

V. Conclusion

The lunar environment is dangerous and unpredictable. Abrasive lunar regolith may wear down exposed surfaces, potentially compromising material integrity. The electrostatic charge and small particle size associated with lunar dust render exposed surfaces difficult to clean. The movement of the insulative Moon through the changing deep space plasma environment and Earth's magnetosphere dynamically charges the lunar regolith. The topography and variable illumination conditions associated with the lunar surface create electric potential differences across areas, inducing low-energy dust transport and lofting phenomena and increasing the probability of arcing. The HLS will sandblast regolith during descent and landing operations, resulting in a cloud of dust that obscures the landing site and abrades the exposed surfaces of the HLS and surface assets. The landing operations will also result in cratering, changing the lunar topography and possibly rendering the lunar surface unstable for later ascent. The sandblasted regolith will remain lofted for a significant time, as the low gravitational force associated with the lunar surface increases particle settling time.

The combination of the dusty surface, dynamically changing plasma environment, and topographical changes must be assessed thoroughly to prevent system failure and ensure crew safety. A detailed risk analysis is required to ensure success in upcoming lunar missions. Experimental simulation of the lunar surface environment is both expensive and technically challenging; current lunar-analogous experiments may not represent the spectrum of charging currents, lunar topography, regolith particle size/morphology distribution, charged vehicle PSIs, the 1/6-g gravitational and vacuum environment on dust dynamics. With powerful modeling tools available, all these factors can be considered simultaneously, increasing the fidelity of lunar mission modeling. We address this need with LSAT, leveraging available simulation programs to create a flexible simulation for lunar surface missions to perform a trade study on these factors from a lunar dust risk perspective, informing mission and system design and decisions within 3-5 years, allowing for the use of this tool for upcoming lunar missions. By utilizing already existing models, the development timeline of LSAT is significantly shortened while a high level of fidelity is maintained. Furthermore, the experimental design for LSAT validation will significantly increase the fundamental understanding of ejecta dynamics in a charged, changing environment. Through utilizing

LSAT during mission logistics planning, landing sites and mission timelines can be determined with a higher level of confidence regarding the lunar dust risks. Overall, LSAT enables a long future of lunar exploration missions.

References

[1] McKay, D. S., Heiken, G., Basu, A., Blanford, G., Simon, S., Reedy, R., French, B. M., and Papike, J., "Lunar Sourcebook: A User's Guide to the Moon," 1991.

[2] Wagner, S., "Asteroid, Lunar and Planetary Regolith Management A Layered Engineering Defense - NASA Technical Reports Server (NTRS)," NTRS - NASA Technical Reports Server. Retrieved 6 July 2022. https://ntrs.nasa.gov/citations/20140011751

[3] Taylor, L., Schmitt, H., Carrier, W., and Nakagawa, M., "Lunar Dust Problem: From Liability to Asset," *1st Space Exploration Conference: Continuing the Voyage of Discovery*, American Institute of Aeronautics and Astronautics, 2005. https://doi.org/10.2514/6.2005-2510

[4] "Apollo 16 Mission Report," MSC-07230, August 1972.

[5] "Apollo 11 Mission Report," NASA-TM-X-62633, November 1969.

[6] Mansfield, C. L., "Apollo 12," NASA, Brian Dunbar, Nov 19 2015. Retrieved 4 September 2022. http://www.nasa.gov/mission_pages/apollo/missions/apollo12.html

[7] "Apollo 15 Mission Report," MSC-05161, December 1971.

[8] Team, Mi. E., "Apollo 17 Mission Report," NASA-TM-X-69292, March 1973.

[9] Linnarsson, D., Carpenter, J., Fubini, B., Gerde, P., Karlsson, L. L., Loftus, D. J., Prisk, G. K., Staufer, U., Tranfield, E. M., and van Westrenen, W., "Toxicity of Lunar Dust," *Planetary and Space Science*, Vol. 74, No. 1, 2012, pp. 57–71. https://doi.org/10.1016/j.pss.2012.05.023

[10] Gaier, J. R., "The Effects of Lunar Dust on EVA Systems During the Apollo Missions," NASA/TM-2005-213610/REV1, April 2007.

[11] Stubbs, T., Halekas, J., Farrell, W., and Vondrak, R., "Lunar Surface Charging: A Global Perspective Using Lunar Prospector Data," *LPI Contributions*, Vol. 1280, 2005.

[12] Deca, J., "Plasma Environment of the Moon," *Encyclopedia of Lunar Science*, edited by B. Cudnik, Springer International Publishing, Cham, 2017, pp. 1–9. https://doi.org/10.1007/978-3-319-05546-6_118-1

[13] Rahimi, A., Ejtehadi, O., Lee, K. H., and Myong, R. S., "Near-Field Plume-Surface Interaction and Regolith Erosion and Dispersal during the Lunar Landing," *Acta Astronautica*, Vol. 175, 2020, pp. 308–326. https://doi.org/10.1016/j.actaastro.2020.05.042

[14] Balakrishnan, K., and Bellan, J., "High-Fidelity Modeling and Numerical Simulation of Cratering Induced by the Interaction of a Supersonic Jet with a Granular Bed of Solid Particles," *International Journal of Multiphase Flow*, Vol. 99, 2018, pp. 1–29. https://doi.org/10.1016/j.ijmultiphaseflow.2017.08.008

[15] You, J., Zhang, X., Zhang, H., Li, C., Xu, Y., Yan, Q., Yu, H., Liu, J., Li, Y., Wang, Y., Zhao, C., Zhang, H., Xu, Y., Chen, L., Lin, H., Fu, Q., Gao, Y., Wang, Y., Wang, W., and Zhi, Q., "Analysis of Plume–Lunar Surface Interaction and Soil Erosion during the Chang'E-4 Landing Process," *Acta Astronautica*, Vol. 185, 2021, pp. 337–351. https://doi.org/10.1016/j.actaastro.2021.05.009

[16] Pirich, R., Weir, J., Leyble, D., Chu, S., and DiGiuseppe, M., "Effects of the Lunar Environment on Space Vehicle Surfaces," presented at the 2010 IEEE Long Island Systems, Applications and Technology Conference, 2010. https://doi.org/10.1109/LISAT.2010.5478329

[17] Hilgers, A., Clucas, S., Thiebault, B., Roussel, J.-F., Mateo-Velez, J.-C., Forest, J., and Rodgers, D., "Modeling of Plasma Probe Interactions With a PIC Code Using an Unstructured Mesh," *IEEE Transactions on Plasma Science*, Vol. 36, No. 5, 2008, pp. 2319–2323. https://doi.org/10.1109/TPS.2008.2003360

[18] Han, D., Wang, J. J., and He, X., "Immersed Finite Element Particle-in-Cell Simulations of Plasma Charging at the Lunar Terminator," *Journal of Spacecraft and Rockets*, Vol. 55, No. 6, 2018, pp. 1490–1497. https://doi.org/10.2514/1.A34002

[19] Cao, Z., White, C., Agir, M. B., and Kontis, K., "Lunar Plume-Surface Interactions Using rarefiedMultiphaseFoam," *Frontiers in Mechanical Engineering*, Vol. 9, 2023. Retrieved 22 February 2024. https://www.frontiersin.org/articles/10.3389/fmech.2023.1116330

[20] Roussel, J.-F., Rogier, F., Dufour, G., Mateo-Velez, J.-C., Forest, J., Hilgers, A., Rodgers, D., Girard, L., and Payan, D., "SPIS Open-Source Code: Methods, Capabilities, Achievements, and

Prospects," *IEEE Transactions on Plasma Science*, Vol. 36, No. 5, 2008, pp. 2360–2368. https://doi.org/10.1109/TPS.2008.2002327
[21] "SPICE Concept." Retrieved 21 February 2024. https://naif.jpl.nasa.gov/naif/spiceconcept.html
[22] "NASA's Plan for Sustained Lunar Exploration and Development," 2020.
[23] Leahy, F. B., "SLS-SPEC-159, Cross-Program Design Specification for Natural Environments (DSNE)," Oct 27 2021.
[24] "LOLA - NASA Science." Retrieved 23 February 2024. https://science.nasa.gov/mission/lro/lola/
[25] Liever, P. A., Gale, M. P., Mehta, R. S., and West, J. S., "Gas-Granular Simulation Framework for Spacecraft Landing Plume-Surface Interaction and Debris Transport Analysis," presented at the Biennial ASCE International Conference on Engineering, Science, Construction and Operations in Challenging Environments (ASCE Earth & Space 2018), Cleveland, OH, 2018.
[26] Veluri, S., Roy, C., Hebert, S., and Luke, E., "Verification of the Loci-CHEM CFD Code Using the Method of Manufactured Solutions," *46th AIAA Aerospace Sciences Meeting and Exhibit*, American Institute of Aeronautics and Astronautics. https://doi.org/10.2514/6.2008-661
[27] Gomez, R., Vicker, D., Rogers, S., Aftosmis, M., Chan, W., Meakin, R., Murman, S., and Murman, S., "STS-107 Investigation Ascent CFD Support," *34th AIAA Fluid Dynamics Conference and Exhibit*, American Institute of Aeronautics and Astronautics, 2004. https://doi.org/10.2514/6.2004-2226
[28] Wang, X., Schwan, J., Hsu, H.-W., Grün, E., and Horányi, M., "Dust Charging and Transport on Airless Planetary Bodies," *Geophysical Research Letters*, Vol. 43, No. 12, 2016, pp. 6103–6110. https://doi.org/10.1002/2016GL069491
[29] Carroll, A., Hood, N., Mike, R., Wang, X., Hsu, H.-W., and Horányi, M., "Laboratory Measurements of Initial Launch Velocities of Electrostatically Lofted Dust on Airless Planetary Bodies," *Icarus*, Vol. 352, 2020, p. 113972. https://doi.org/10.1016/j.icarus.2020.113972
[30] Yeo, L. H., Wang, X., Deca, J., Hsu, H.-W., and Horányi, M., "Dynamics of Electrostatically Lofted Dust on Airless Planetary Bodies," *Icarus*, Vol. 366, 2021, p. 114519. https://doi.org/10.1016/j.icarus.2021.114519
[31] "ARES | Exploration Science Projects | Lunar Regolith Simulants | Glenn Research Center (GRC)." Retrieved 16 May 2024. https://ares.jsc.nasa.gov/projects/simulants/dust-testing-facilities/glenn-research-center.html
[32] Wang, J., and Huang, Z., "Dusty Spacesuit Charging/Arcing in Plasma: Implications for Astronaut Safety at the Lunar Terminator and Far-Side," presented at the AGU Fall Meeting 2019, 2019.
[33] Halekas, J. S., Delory, G. T., Lin, R. P., Stubbs, T. J., and Farrell, W. M., "Lunar Prospector Observations of the Electrostatic Potential of the Lunar Surface and Its Response to Incident Currents," *Journal of Geophysical Research: Space Physics*, Vol. 113, No. A9, 2008. https://doi.org/10.1029/2008JA013194
[34] "IM-1," Intuitive Machines. Retrieved 29 February 2024. https://www.intuitivemachines.com/im-1
[35] Barker, M. K., Mazarico, E., Neumann, G. A., Smith, D. E., Zuber, M. T., and Head, J. W., "Improved LOLA Elevation Maps for South Pole Landing Sites: Error Estimates and Their Impact on Illumination Conditions," *Planetary and Space Science*, Vol. 203, 2021, p. 105119. https://doi.org/10.1016/j.pss.2020.105119
[36] Hebeler, F., "Hillshade," MATLAB Central File Exchange. https://www.mathworks.com/matlabcentral/fileexchange/14863-hillshade
[37] "Moon's South Pole Is Full of Mystery, Science, Intrigue - NASA," Aug 18 2022. Retrieved 5 June 2024. https://www.nasa.gov/humans-in-space/moons-south-pole-is-full-of-mystery-science-intrigue/
[38] "SpaceX," SpaceX. Retrieved 4 September 2022. http://www.spacex.com
[39] Vaidheeswaran, A., Gel, A., Clarke, M., and Rogers, W., "Sensitivity Analysis of Particle-In-Cell Modeling Parameters in Settling Bed, Bubbling Fluidized Bed and Circulating Fluidized Bed," DOE/NETL--2021/2642, 1756845, January 2021, p. DOE/NETL--2021/2642, 1756845. https://doi.org/10.2172/1756845

[40] “NASA Identifies Candidate Regions for Landing Next Americans on Moon - NASA.” Retrieved 23 May 2024. https://www.nasa.gov/news-release/nasa-identifies-candidate-regions-for-landing-next-americans-on-moon/
[41] “Project Cost Estimating Capability (PCEC)(MFS-33187-2) | NASA Software Catalog.” Retrieved 29 February 2024. https://software.nasa.gov/software/MFS-33187-2
[42] Rubio, J. S., Gorman, M., Diaz-Lopez, M. X., and Ni, R., “Plume-Surface Interaction Physics Focused Ground Test 1: Setup and Preliminary Results,” *AIAA SCITECH 2022 Forum*, American Institute of Aeronautics and Astronautics. https://doi.org/10.2514/6.2022-1809